Selective control of type I IFN induction by the Rac activator DOCK2 during TLR-mediated plasmacytoid dendritic cell activation

Kazuhito Gotoh,[1,3] Yoshihiko Tanaka,[1,4] Akihiko Nishikimi,[1,4] Risa Nakamura,[2] Hisakata Yamada,[2] Naoyoshi Maeda,[2] Takahiro Ishikawa,[2] Katsuaki Hoshino,[5] Takehito Uruno,[1] Qinhong Cao,[1] Sadayuki Higashi,[1,4] Yasushi Kawaguchi,[6] Munechika Enjoji,[3] Ryoichi Takayanagi,[3] Tsuneyasu Kaisho,[5] Yasunobu Yoshikai,[2] and Yoshinori Fukui[1,4]

[1]Division of Immunogenetics, Department of Immunobiology and Neuroscience, [2]Division of Host Defense, Research Center for Prevention of Infectious Diseases, Medical Institute of Bioregulation, and [3]Department of Medicine and Bioregulatory Science, Graduate School of Medical Sciences, Kyushu University, Fukuoka 812-8582, Japan
[4]Japan Science and Technology Agency, Core Research for Evolutional Science and Technology, Tokyo 102-0075, Japan
[5]Laboratory for Host Defense, RIKEN Research Center for Allergy and Immunology, Kanagawa 230-0045, Japan
[6]Division of Viral Infection, Department of Infectious Disease Control, International Research Center for Infectious Diseases, Institute of Medical Science, University of Tokyo, Tokyo 108-8639, Japan

Plasmacytoid dendritic cells (pDCs) play a key role in antiviral immunity, but also contribute to the pathogenesis of certain autoimmune diseases, by producing large amounts of type I IFNs. Although activation of pDCs is triggered by engagement of nucleotide-sensing toll-like receptors (TLR) 7 and 9, type I IFN induction additionally requires IκB kinase (IKK) α–dependent activation of IFN regulatory factor (IRF) 7. However, the signaling pathway mediating IKK-α activation is poorly defined. We show that DOCK2, an atypical Rac activator, is essential for TLR7- and TLR9-mediated IFN-α induction in pDCs. We found that the exposure of pDCs to nucleic acid ligands induces Rac activation through a TLR-independent and DOCK2-dependent mechanism. Although this Rac activation was dispensable for induction of inflammatory cytokines, phosphorylation of IKK-α and nuclear translocation of IRF-7 were impaired in *Dock2*-deficient pDCs, resulting in selective loss of IFN-α induction. Similar results were obtained when a dominant-negative Rac mutant was expressed in wild-type pDCs. Thus, the DOCK2–Rac signaling pathway acts in parallel with TLR engagement to control IKK-α activation for type I IFN induction. Owing to its hematopoietic cell–specific expression, DOCK2 may serve as a therapeutic target for type I IFN–related autoimmune diseases.

CORRESPONDENCE
Yoshinori Fukui:
fukui@bioreg.kyushu-u.ac.jp

Abbreviations used: DOTAP, 1,2-dioleoyloxy-3-trimethylammonium-propane; GEF, guanine nucleotide exchange factor; IKK, IκB kinase; IRAK, IL-1 receptor–associated kinase; IRF, IFN regulatory factor; MOI, multiplicity of infection; pDC, plasmacytoid DC; TfR, transferrin receptor; TLR, toll-like receptor.

Plasmacytoid DCs (pDCs) represent a specialized DC population that is capable of producing large amounts of type I IFNs (IFN-α and IFN-β) for antiviral immunity (Gilliet et al., 2008). Activation of pDCs is mediated by toll-like receptors (TLRs) 7 and 9, intracellular receptors which recognize single-stranded RNA or unmethylated CpG DNA, respectively (Hemmi et al., 2000; Jarrossay et al., 2001; Diebold et al., 2004; Heil et al., 2004). Upon binding of their ligands, both TLR7 and TLR9 recruit a cytoplasmic adaptor MyD88, downstream of which the signaling pathways are bifurcated to induce either inflammatory

cytokines or type I IFNs (Akira et al., 2006). In pDCs, induction of type I IFNs critically depends on IFN regulatory factor (IRF) 7 (Honda et al., 2005b). IRF-7 makes a complex with MyD88, TNF receptor–associated factor 6, and IL-1 receptor–associated kinases (IRAKs) and translocates to the nucleus upon phosphorylation (Kawai et al., 2004; Uematsu et al., 2005). Although recent evidence indicates that IκB kinase (IKK) α directly binds to and activates IRF-7 (Hoshino et al., 2006),

K. Gotoh and Y. Tanaka contributed equally to this paper.

721

The Journal of Experimental Medicine

the signaling cascades leading to type I IFN induction are not completely defined. Elucidation of this regulatory mechanism would be clinically important because type I IFNs produced by pDCs have been implicated in the pathogenesis of autoimmune diseases such as psoriasis and systemic lupus erythematosus (Blanco et al., 2001; Nestle et al., 2005; Lande et al., 2007).

Rac is a member of the Rho family of GTPases that function as molecular "switches" by cycling GDP-bound inactive states and GTP-bound active states. Once activated, Rac interacts with multiple downstream effectors to regulate various cellular functions including actin reorganization and gene expression. Stimulus-induced formation of the active GTP-bound Rac is mediated by guanine nucleotide exchange factors (GEFs). DOCK2 is a member of the CDM family of proteins (*Caenorhabditis elegans* CED-5, mammals DOCK180, and *Drosophila melanogaster* myoblast city) and is predominantly expressed in hematopoietic cells (Reif and Cyster, 2002). Although DOCK2 does not contain the Dbl homology domain and the pleckstrin homology domain that are typically found in GEFs, DOCK2 catalyzes the GTP–GDP exchange reaction for Rac via its Docker (also known as DHR-2) domain (Brugnera et al., 2002; Côté and Vuori, 2002). There is accumulating evidence that DOCK2 functions downstream of chemokine receptors and regulates migration of certain subsets of immune cells (Fukui et al., 2001; Nombela-Arrieta et al., 2004, 2007; Kunisaki et al., 2006; Shulman et al., 2006; Nishikimi et al., 2009). Indeed, pDCs, but not myeloid DCs, from *Dock2*-deficient (*Dock2*$^{-/-}$) mice exhibit a severe defect in chemokine-induced Rac activation, resulting in reduction of motility and the loss of polarity during chemotaxis (Gotoh et al., 2008). Thus, DOCK2 is a major Rac GEF that controls migration of pDCs. However, the role of DOCK2 in TLR-mediated pDC activation remains unknown.

In this paper, we present evidence that DOCK2 controls TLR7- and TLR9-mediated IFN-α induction in pDCs via Rac activation. This Rac activation occurred independently of TLR engagement but was critically required for TLR-mediated IKK-α activation and type I IFN induction. Our results thus define a novel regulatory mechanism controlling type I IFN induction in pDCs.

RESULTS AND DISCUSSION
DOCK2 is required for TLR7/9–mediated type I IFN induction in pDCs

To examine the role of DOCK2 in TLR-mediated cytokine production, we first measured serum IFN-α and IL-12p40 after intravenously injecting TLR ligands into WT and *Dock2*$^{-/-}$ mice. When A-type CpG DNA (D19), a TLR9 ligand (Verthelyi et al., 2001), was administrated, both WT and *Dock2*$^{-/-}$ mice comparably produced IL-12p40 (Fig. 1 A). Similar results were obtained with a TLR7 ligand R848 (Fig. 1 A; Hemmi et al., 2002), indicating that DOCK2 deficiency does not affect TLR7/9-mediated inflammatory cytokine production. Surprisingly, however, both CpG-A and R848 failed to induce IFN-α production in *Dock2*$^{-/-}$ mice (Fig. 1 A).

Although pDCs are normally generated in the BM in the absence of DOCK2, *Dock2*$^{-/-}$ mice exhibit a severe reduction of pDCs in the spleen and lymph nodes (Gotoh et al., 2008). Therefore, this mislocalization of pDCs may have affected TLR7/9-mediated IFN-α production in vivo. To determine more precisely the role of DOCK2 in type I IFN induction, we purified pDCs from Flt3 ligand–induced BM-derived DCs and stimulated them in vitro with CpG-A, R848, and another TLR9 ligand CpG-B (1668; Krieg et al., 1995). Although WT pDCs produced considerable amounts of IFN-α and IFN-β in response to these TLR ligands, TLR7/9-mediated type I IFN induction was severely impaired in *Dock2*$^{-/-}$ pDCs (Fig. 1, B–D). Similar results were obtained when naive BM pDCs were stimulated with CpG-A (Fig. 1 E). In contrast, induction of IL-12p40 and IL-6 and up-regulation of costimulatory molecules occurred normally in *Dock2*$^{-/-}$ pDCs (Fig. 1 F and not depicted). These results indicate that DOCK2 selectively controls type I IFN induction pathway during TLR7/9-mediated pDC activation.

Influenza A virus and HSV type 2 (HSV-2) are known to activate the TLR7 and TLR9 signaling pathways, respectively (Lund et al., 2003; Diebold et al., 2004). To examine whether DOCK2 is also important for virus-induced IFN-α production, WT and *Dock2*$^{-/-}$ pDCs were stimulated with these viruses in vitro. Although WT pDCs produced large amounts of IFN-α depending on a multiplicity of infection (MOI), production of IFN-α by *Dock2*$^{-/-}$ pDCs was markedly suppressed at any MOIs tested (Fig. 1 G). Similar results were obtained when heat- or UV-inactivated virus and purified HSV-2 DNA were used (Fig. 1, H and I), indicating that DOCK2 controls IFN-α induction independently of virus replication. In contrast, such a drastic difference was not found in IL-12p40 production, although *Dock2*$^{-/-}$ pDCs produced less IL-12p40 than WT pDCs at a certain MOI (Fig. 1 G).
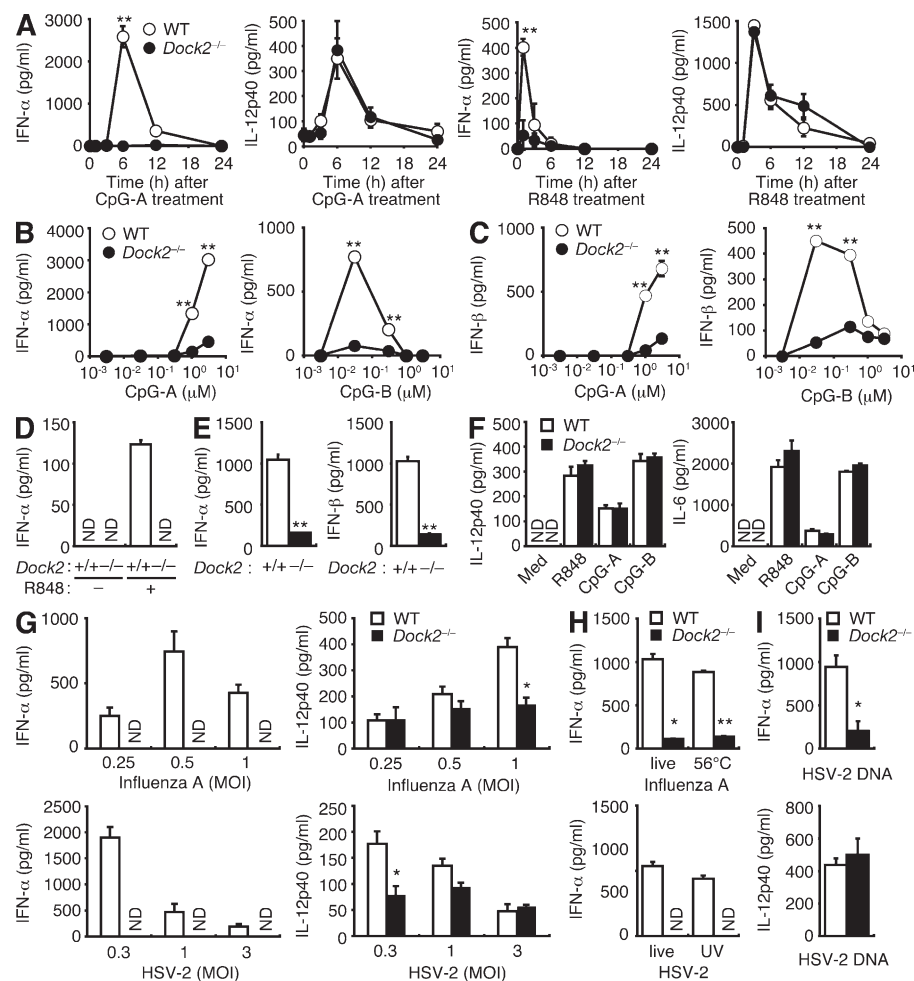
DOCK2 controls TLR7/9–mediated type I IFN induction via Rac activation

To explore the mechanism by which DOCK2 controls type I IFN induction, we first compared ligand uptake between WT and *Dock2*$^{-/-}$ pDCs. The Cy5-labeled CpG-A was comparably incorporated into both types of pDCs (Fig. 2 A), indicating that DOCK2 deficiency does not affect CpG-A uptake. However, although WT pDCs exhibited a localized accumulation of F-actin in response to CpG-A, F-actin assembly was scarcely found in *Dock2*$^{-/-}$ pDCs (Fig. 2 B). Because the morphological change was induced in WT pDCs treated with CpG-A–coated beads (Fig. 2 C), this actin polymerization, as previously suggested in macrophages (Sanjuan et al., 2006), appeared to be triggered at the cell surface, independently of TLR9 engagement. Indeed, after CpG-A stimulation, *Tlr9*$^{-/-}$ pDCs also exhibited polarized morphology with focused distribution of F-actin (Fig. 2 B). In human pDCs, it has been reported that CXCL16, a scavenger receptor, recognizes CpG-A at the cell surface and mediates its uptake (Gursel et al., 2006). However, CXCL16 deficiency did not affect CpG-A uptake, actin polymerization,

and IFN-α induction in mouse pDCs (Fig. S1, A–C). In addition, CpG-A uptake and actin polymerization were insensitive to pertussis toxin and the Src family kinase inhibitor PP2 (Fig. S1, D and E), ruling out the possible involvement of G protein–coupled receptors and tyrosine kinase signaling pathways in these cellular functions, although treatment with PP2, but not pertussis toxin, inhibited induction of both IFN-α and IL-12p40 in WT pDCs (Fig. S1 F).

Having found that CpG-A induces actin polymerization in TLR9-independent and DOCK2-dependent mechanisms, we compared Rac activation among WT, $Tlr9^{-/-}$, and $Dock2^{-/-}$ pDCs. In response to CpG-A, Rac was activated in $Tlr9^{-/-}$ pDCs to the same extent and at the same

kinetics as in WT pDCs (Fig. 2 D). However, CpG-A–induced Rac activation was almost totally abolished in $Dock2^{-/-}$ pDCs (Fig. 2 D). This defect in Rac activation was also observed when $Dock2^{-/-}$ pDCs were stimulated with other TLR ligands such as R848, influenza A virus, HSV-2, and purified HSV-2 DNA (Fig. 2, E–G). In contrast, Rac activation and actin polymerization occurred normally in $Dock2^{-/-}$ myeloid DCs stimulated with CpG-A (Fig. S2), indicating that the effect of DOCK2 deficiency on TLR ligand–induced Rac activation is limited to pDCs. To directly examine whether Rac activation is involved in type I IFN induction in pDCs, we retrovirally transduced WT pDCs to express a dominant-negative Rac mutant

Figure 1. DOCK2 is required for TLR7/9–mediated type I IFN induction in pDCs. (A) Serum IFN-α and IL-12p40 levels were compared between WT and $Dock2^{-/-}$ mice after injection of CpG-A complexed with the cationic lipids DOTAP (left) or R848 (right). Data are the mean ± SD of three mice, and are representative of two independent experiments. **, P < 0.001. (B–I) The levels of IFN-α (B, D, E, G, H, and I), IFN-β (C and E), IL-12p40 (F, G, and I), and IL-6 (F) in cell culture supernatants were compared between WT and $Dock2^{-/-}$ pDCs 24 h after stimulation with TLR7 or TLR9 ligands. Data are expressed as the mean ± SD of triplicate wells and are representative of three (B–G) or two (H and I) independent experiments. **, P < 0.001; *, P < 0.01. ND indicates below the detectable limit. (B, C, D, and F) Flt3 ligand–induced BM–derived pDCs (4×10^4 cells per well) were stimulated with CpG-A (B and C, 0–3 μM; F, 3 μM), CpG-B (B and C, 0–3 μM; F, 1 μM), or R848 (D and F, 100 nM). (E) Naive BM pDCs (4×10^4 cells per well) were stimulated with CpG-A (3 μM). (G) Flt3 ligand–induced BM–derived pDCs (2×10^5 cells per well) were infected with influenza A virus or HSV-2 at the indicated MOIs. (H) Flt3 ligand–induced BM-derived pDCs (2×10^5 cells per well) were stimulated with live or inactivated influenza A virus or HSV-2 at an MOI of 0.5 or 0.3, respectively. (I) Flt3 ligand–induced BM-derived pDCs (4×10^5 cells per well) were stimulated with 2.74 μg/ml HSV-2 DNA.

(T17N-Rac). Compared with the cells expressing the WT Rac control, the expression of T17N-Rac markedly suppressed CpG-A–induced IFN-α production without affect-ing IL-12p40 levels (Fig. 2 H). Similarly, the expression of T17N-Rac abrogated influenza A virus–mediated induction of IFN-α, but not IL-12p40, in WT pDCs (Fig. 2 I). These
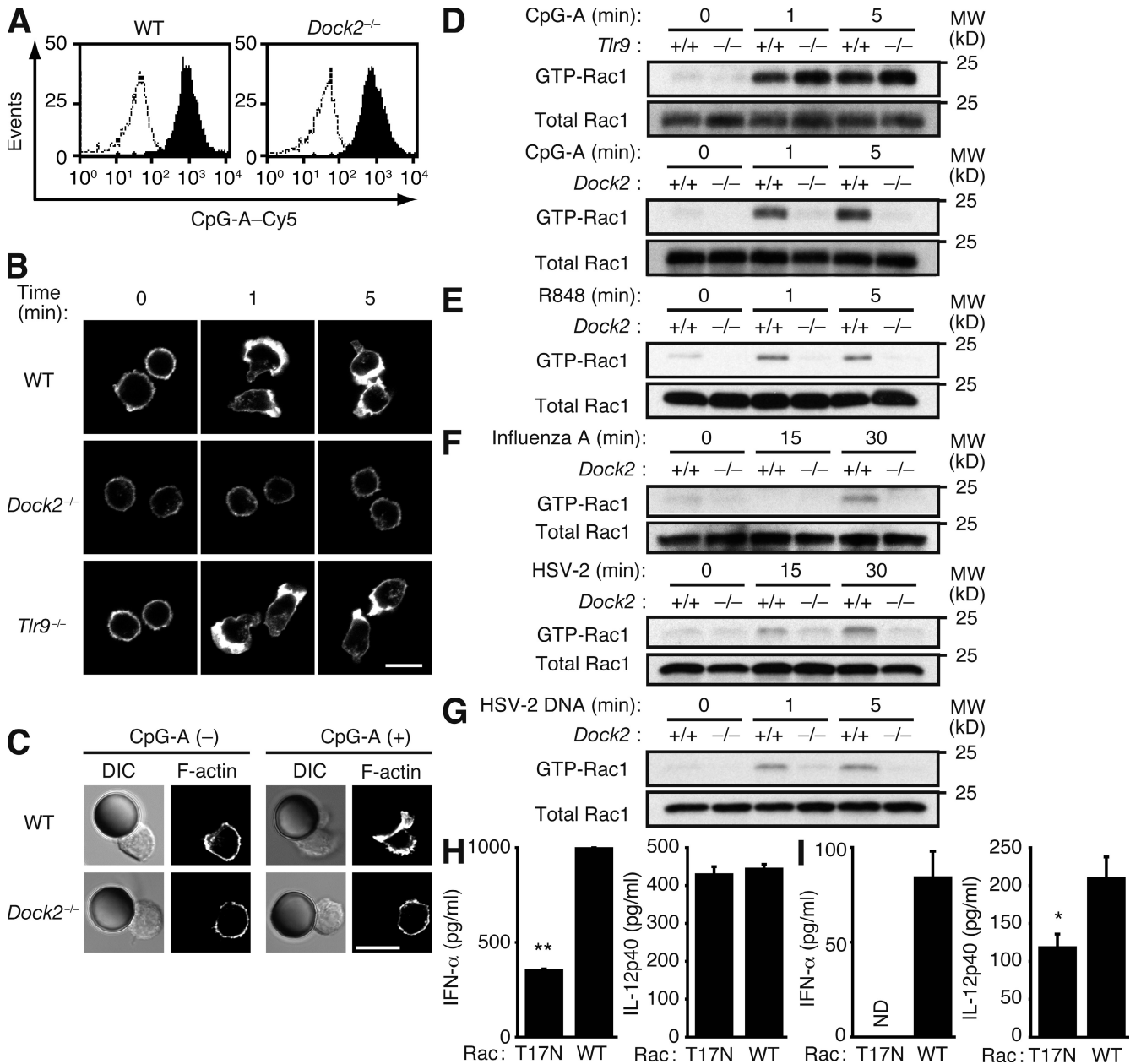
Figure 2. DOCK2 controls TLR7/9–mediated type I IFN induction in pDCs via Rac activation. (A) The uptake of CpG-A was compared between WT and Dock2$^{-/-}$ pDCs after cells were incubated with 3 µM CpG-A–Cy5 at 37°C (filled area) or 4°C (open area) for 1 h. Before assay, cell surface fluores-cence was quenched with 0.2% trypan blue. Representative profiles of three independent experiments are shown. (B and C) BM-derived pDCs from WT, Dock2$^{-/-}$, and Tlr9$^{-/-}$ mice were stimulated with 3 µM CpG-A for the indicated times (B) or CpG-A–coated polystyrene beads for 1 min (C). Cells were then fixed and stained with phalloidin. Representative images of two independent experiments are shown. DIC, differential interference contrast. Bars, 10 µm. (D–G) Activation of Rac was analyzed for BM-derived pDCs from WT (+/+), Dock2$^{-/-}$, and Tlr9$^{-/-}$ mice after stimulation with 3 µM CpG-A (D), 100 nM R848 (E), influenza A virus, or HSV-2 at a MOI of 0.5 (F) or 2.18 µg/ml HSV-2 DNA (G) for the indicated times. Data are representative of three (D and F) or two (E and G) independent experiments. (H and I) BM-derived WT pDCs were retrovirally transduced to express either T17N-Rac–IRES–GFP or WT Rac–IRES–GFP. After fluorescence-activated cell sorting, GFP-positive cells (H, 4 × 10⁴ cells per well; I, 6 × 10⁴ cells per well) were stimulated with 3 µM CpG-A (H) or influenza A virus at an MOI of 0.5 (I) for 24 h. Data indicate the levels of IFN-α and IL-12p40 in cell culture supernatants (mean ± SD of triplicate wells) and are representative of five (H) and two (I) independent experiments. **, P < 0.001; *, P < 0.01. ND indicates below the detectable limit.

results indicate that DOCK2 controls TLR7/9-mediated type I IFN induction in pDCs through Rac activation.

Type I IFN signaling and TLR engagement are unaffected in *Dock2*$^{-/-}$ pDCs

Although activation of basally expressed IRF-7 induces type I IFN gene expression, robust type I IFN production requires IFN signal–dependent IRF-7 expression. This positive-feedback regulation involves a complex called IFN-stimulated gene factor 3, which is composed of STAT-1, STAT-2, and IRF-9 (Honda et al., 2006). As CpG-A–mediated *Irf7* induction was significantly reduced in *Dock2*$^{-/-}$ pDCs at 3 h after stimulation (Fig. 3 A), we examined whether DOCK2 functions downstream of type I IFN receptors. Although CpG-A–induced STAT-1 phosphorylation was impaired in *Dock2*$^{-/-}$ pDCs (Fig. 3 B), STAT-1 was normally phosphorylated in these cells in response to IFN-α (Fig. 3 C). Consistent with this finding, the expression of *Irf7* and *Cxcl10*, another IFN-inducible gene, were comparably up-regulated in WT and *Dock2*$^{-/-}$ pDCs after stimulation with IFN-α (Fig. 3 D). These results suggest that DOCK2 controls the initial IFN induction pathway rather than the IFN signal–dependent positive-feedback loop.

Both TLR7 and TLR9 reside in the ER and are recruited to endolysosomes upon stimulation to detect internalized ligands (Latz et al., 2004; Leifer et al., 2004). As TLR9 engagement by CpG-A in early endosomes is suggested to be important for robust type I IFN induction (Honda et al., 2005a; Guiducci et al., 2006), we examined whether DOCK2 deficiency alters subcellular localization of TLR9 and CpG-A. Although the majority of YFP-tagged TLR9 was localized in the ER under unstimulated conditions, this proportion was markedly reduced upon stimulation, irrespective of DOCK2 expression (Fig. 3 E). More importantly, in WT and *Dock2*$^{-/-}$ pDCs, TLR9-YFP and CpG-A–Cy5 comparably accumulated in the transferrin receptor (TfR)–positive endosomal compartments at 1.5 and 6 h after stimulation (Fig. 3 F), indicating that DOCK2 deficiency does not interfere with TLR engagement in early endosomes. When LAMP-1–positive late endosomes/lysosomes were analyzed, the proportion of TLR9 and CpG-A colocalized with LAMP-1 somewhat decreased in *Dock2*$^{-/-}$ pDCs at 6 h, compared with that in WT pDCs (Fig. 3 G). Although the precise meaning of this difference remains unknown, it seems unlikely that this difference directly affects the ability of IFN-α induction because such a difference was not found when WT and *Dock2*$^{-/-}$ pDCs were stimulated with CpG-B (Fig. S3).

DOCK2–mediated Rac activation is critical for IKK-α activation in pDCs

Having found that TLR engagement in early endosomes is unaffected in the absence of DOCK2, we next examined the nuclear translocation of IRF-7 by staining pDCs with anti–IRF-7 antibody and DAPI. Although IRF-7 was expressed in the cytoplasm of unstimulated pDCs, stimulation with CpG-A induced nuclear accumulation of IRF-7 in WT,

but not *Dock2*$^{-/-}$, pDCs (Fig. 4 A). Recent evidence indicates that PI3Ks (phosphatidylinositol-3 kinases) control the nuclear translocation of IRF-7 (Guiducci et al., 2008). However, phosphorylation of Akt, a downstream effector of PI3Ks, as well as that of ERK, JNK, and p38 occurred normally in *Dock2*$^{-/-}$ pDCs stimulated with CpG-A (Fig. 4 B). Similarly, DOCK2 deficiency did not affect CpG-A–induced degradation and autophosphorylation of IRAK-1, which is also essential for IRF-7 activation (Fig. 4, C and D; Uematsu et al., 2005).

IKK–α is involved in phosphorylation and nuclear translocation of IRF-7 (Hoshino et al., 2006). IKK–α carries two serine residues at positions 176 and 180 in the activation loop, which are phosphorylated during cellular stimulation (Häcker and Karin, 2006). In WT pDCs, IKK–α was phosphorylated at these sites in response to CpG-A (Fig. 4 E). However, such phosphorylation was hardly detected in both *Dock2*$^{-/-}$ and *Tlr9*$^{-/-}$ pDCs (Fig. 4, E and F). Moreover, IKK–α phosphorylation was inhibited in WT pDCs by treating them with a cell-permeable dominant–negative Rac mutant (Tat–T17N–Rac; Fig. 4 G). A critical role of this IKK–α phosphorylation in type I IFN induction was examined by luciferase assays. Overexpression of MyD88 augmented IRF-7–induced *Ifna* promoter activation (Fig. S4). This augmentation was inhibited by coexpression of an IKK–α mutant encoding alanines instead of serines at positions 176 and 180 (IKK–α SSAA) as well as a kinase-inactive IKK–α mutant (Fig. S4). Conversely, *Ifna* promoter activation was further enhanced by coexpression of an IKK–α mutant with glutamates at these sites (IKK–α SSEE), which mimics the effect of phosphorylated serines (Fig. S4). Collectively, these results suggest that DOCK2-mediated Rac activation controls type I IFN induction, at least in part, through phosphorylation and activation of IKK–α.

In this paper, we have provided evidence that DOCK2 couples ligand stimulation to type I IFN induction in pDCs via Rac activation. We found that the exposure of pDCs to nucleic acid ligands induces Rac activation through a TLR-independent and DOCK2-dependent mechanism. This Rac activation was not required for TLR engagement in early endosomes and IFN signal–dependent positive feedback regulation. However, TLR–mediated IKK–α activation was severely impaired in pDCs lacking DOCK2 and those expressing a dominant-negative Rac mutant, resulting in selective loss of type I IFN induction in these cells. Our results thus indicate that the DOCK2–Rac signaling pathway acts in parallel with TLR engagement to control IKK–α activation for type I IFN induction. Although the precise mechanism by which Rac controls IKK–α activation is currently unknown, it has been reported that activation of IKK complex is regulated by a redox-dependent mechanism in other receptor systems (Oakley et al., 2009). As Rac is a cytosolic component of the NADPH (nicotinamide adenine dinucleotide phosphate) oxidase, Rac may therefore control IKK–α activation through generation of reactive oxygen species. Alternatively, PAK (p21-activated kinase), a downstream

effector of Rac, may be directly or indirectly involved in IKK-α activation, as was previously reported for other IKKs (Cammarano and Minden, 2001; Ehrhardt et al., 2004). Further studies will be required to determine how IKK-α activation is controlled by Rac in pDCs.

Although pDCs play a key role in antiviral immunity, there is growing evidence that pDCs also contribute to the pathogenesis of autoimmune diseases by producing large amounts of type I IFNs. Thus far, several molecules, including IKK-α and IRF-7, have been shown to control type I
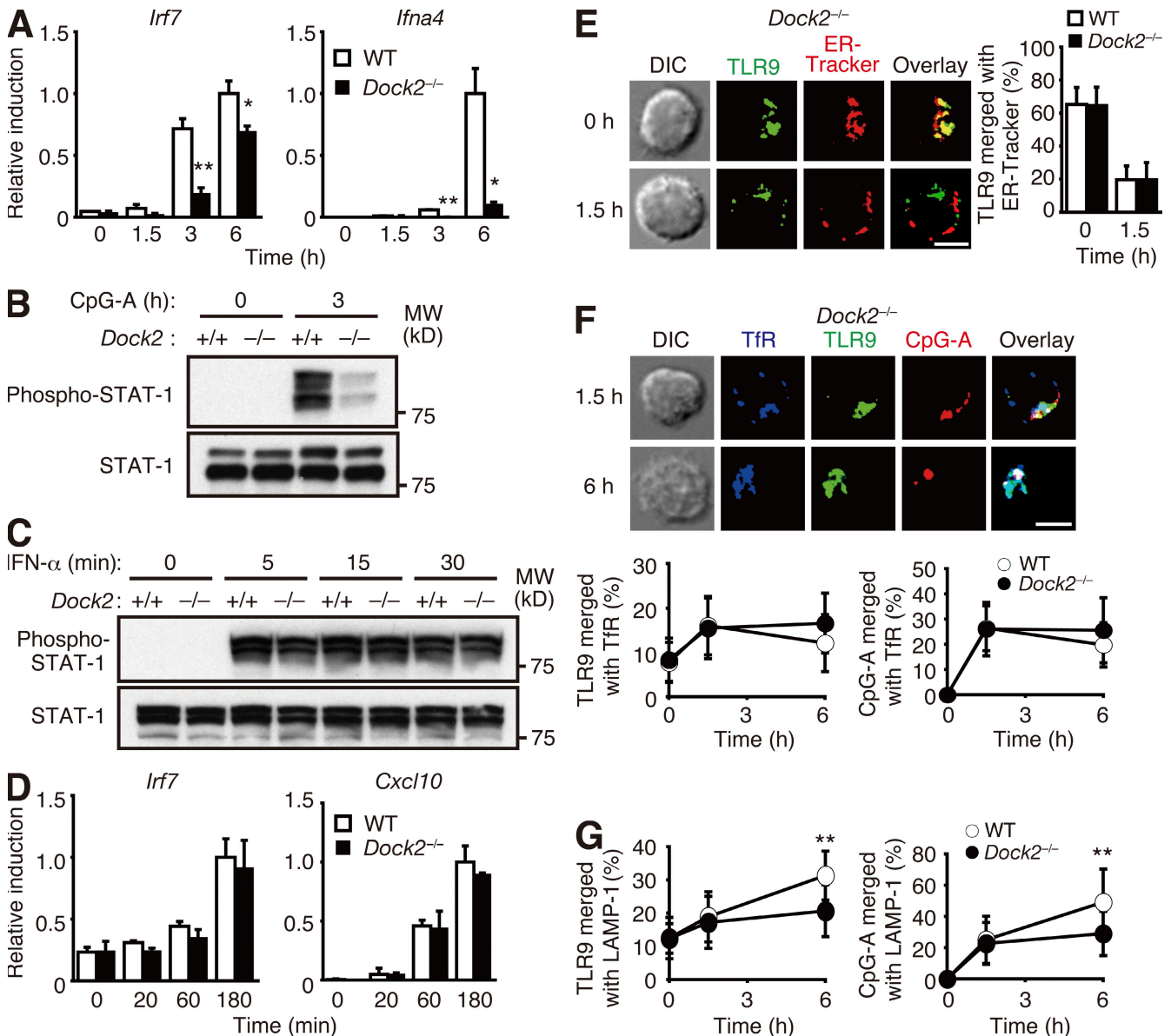
Figure 3.   Type I IFN signaling and TLR engagement in early endosomes are unaffected in the absence of DOCK2. (A) Real-time PCR analysis of *Irf7* and *Ifna4* expression in BM-derived pDCs stimulated with 3 μM CpG-A for the indicated times. Data are expressed as the mean ± SD of triplicate reactions after normalization to expression of the gene encoding hypoxanthine guanine phosphoribosyl transferase 1 (*Hprt1*) and are representative of two independent experiments. **, P < 0.001; *, P < 0.01. (B and C) BM-derived WT and *Dock2⁻/⁻* pDCs were stimulated with 3 μM CpG-A (B) or 500 U/ml IFN-α (C) for the indicated times and analyzed for phosphorylation of STAT-1. Data are representative of three (B) and two (C) independent experiments. (D) Real-time PCR analysis of *Irf7* and *Cxcl10* expression in BM-derived pDCs stimulated with 500 U/ml IFN-α for the indicated times. Data are expressed as the mean ± SD of triplicate reactions after normalization to *Hprt1* expression and are representative of two independent experiments. (E–G) BM-derived pDCs retrovirally transduced with TLR9–YFP were stimulated with 3 μM CpG-A for the indicated times. After fixation, cells were stained with ER-Tracker (E), anti–TfR antibody (F), or anti–LAMP-1 antibody (G). The area of TLR9-YFP or CpG-A–Cy5 merged with ER-Tracker (E), TfR (F), or LAMP-1 (G) was calculated in each cell. Bars, 5 μm. (E) Data are expressed as the percentage of colocalization (mean ± SD; *n* = 10) and are representative of two independent experiments. (F and G) Data were pooled from three independent experiments and are expressed as the percentage of colocalization (mean ± SD) for 30 cells analyzed per group. **, P < 0.001.

IFN induction in pDCs. However, their ubiquitous expression precludes the use as therapeutic targets. Unlike these molecules, DOCK2 expression is limited to hematopoietic cells (Fukui et al., 2001). In addition, we have demonstrated in this paper that DOCK2 selectively controls type I IFN induction during TLR7/9–mediated pDC activation. Therefore, DOCK2 may be a novel therapeutic target for controlling type I IFN–related autoimmune diseases.

MATERIALS AND METHODS

Mice. *Dock2*−/−, *Tlr9*−/−, and *Cxcl16*−/− mice have been described elsewhere (Hemmi et al., 2000; Fukui et al., 2001; Shimaoka et al., 2007). *Dock2*−/− mice were backcrossed with C57BL/6 mice for more than eight generations before use. *Tlr9*−/− mice and *Cxcl16*−/− BM cells were provided by S. Akira

(Osaka University, Osaka, Japan) and S. Ueha and K. Matsushima (both from the University of Tokyo, Tokyo, Japan), respectively. Age-matched and sex-matched C57BL/6 mice were used as WT controls. Mice were kept under specific pathogen-free conditions in the animal facility of Kyushu University. Animal protocols were approved by the committee of Ethics on Animal Experiment, Faculty of Medical Sciences, Kyushu University.

Reagents. The following CpG oligonucleotides were synthesized at Hokkaido System Science: CpG-A (D19), ggTGCATCGATGCAgggggG; and CpG-B (1668), tccatgacgttcctgatgct (uppercase and lowercase letters indicate bases with phosphodiester- and phosphorothioate-modified backbones, respectively). The Cy5-labeled CpG-A and CpG-B were obtained from Sigma-Aldrich. R848 was purchased from Enzo Life Sciences, Inc., and pertussis toxin and PP2 were obtained from EMD. For viral infection, HSV-2 (186 strain) and influenza A/New Caledonia/20/99 (H1N1) were used.
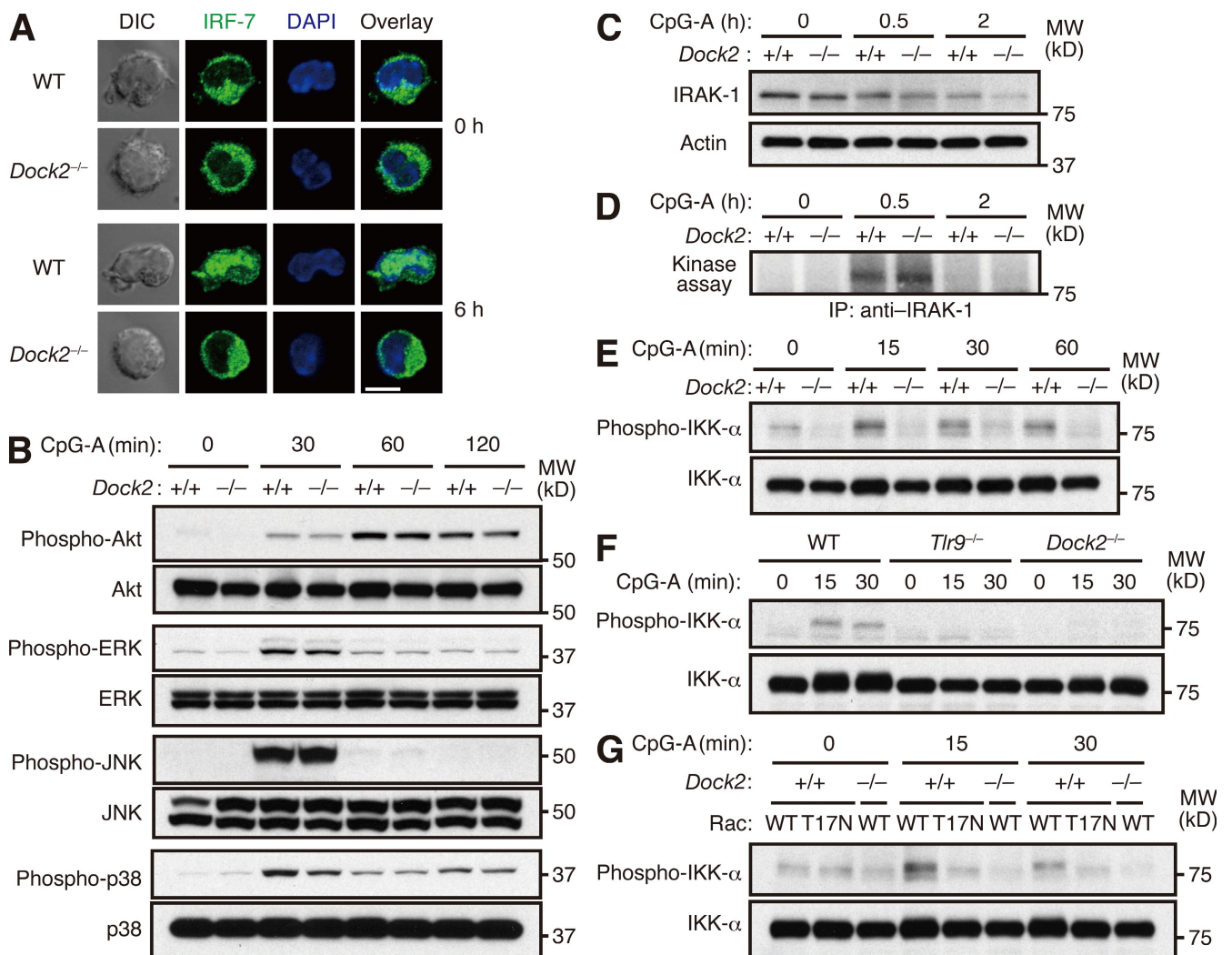
Figure 4. DOCK2–mediated Rac activation is critical for IKK–α activation in pDCs. (A) Subcellular localization of IRF-7 was compared between WT and *Dock2*−/− pDCs after stimulation with CpG-A. DAPI was used to stain nuclei. Representative images of three independent experiments are shown. Bar, 5 μm. (B) BM-derived pDCs from WT and *Dock2*−/− mice were stimulated with 3 μM CpG-A for the indicated times and analyzed for phosphorylation of Akt, ERK, JNK, or p38. Data are representative of at least two independent experiments. (C and D) BM-derived WT and *Dock2*−/− pDCs were stimulated with 3 μM CpG-A for the indicated times and analyzed for the expression (C) and autophosphorylation (D) of IRAK-1. Data are representative of two independent experiments. (E–G) BM-derived pDCs from WT, *Dock2*−/−, and *Tlr9*−/− mice were stimulated with 3 μM CpG-A for the indicated times and analyzed for serine phosphorylation of IKK–α at positions 176 and 180. (G) Before stimulation, cells were treated with bacterially expressed GFP-tagged Tat–T17N-Rac or Tat–WT Rac (500 nM each) for 30 min at 37°C. Data are representative of three (E and G) or two (F) independent experiments.

In some experiments, the virus was used for stimulation after inactivation by exposure to 1 J/cm² UV light with a UV cross-linker or incubation at 56°C for 30 min. HSV-2 186 viral DNA was purified on 5–20% potassium acetate gradient. Cytokine ELISA kits were purchased from R&D Systems (IFN-α and IFN-β) and Thermo Fisher Scientific (IL-12p40 and IL-6).

In vivo treatment. Mice were anesthetized and intravenously injected with 200 µl R848 (50 nmol) or CpG-A complexed with the cationic lipid 1,2-dioleoyloxy-3-trimethylammonium-propane (DOTAP). For preparation of CpG-A/DOTAP mixture, 5 µg CpG-A resolved in 50 µl PBS was incubated with 30 µl (30 µg) of DOTAP Liposomal Transfection Reagent (Roche) in a polystyrene tube containing 70 µl PBS for 15 min at room temperature. The sample was then diluted with 50 µl PBS to make 200 µl of CpG-A/DOTAP mixture.

Cell preparation and retrovirus-mediated gene transfer. Flt3 ligand–induced BM-derived pDCs, GM-CSF–induced BM-derived myeloid DCs, and naive BM pDCs were prepared as described elsewhere (Gotoh et al., 2008). The retroviral vector pMX (provided by T. Kitamura, University of Tokyo, Tokyo, Japan) was used to generate the plasmid encoding TLR9-YFP, T17N-Rac–IRES–GFP, or WT Rac–IRES–GFP. These plasmids were transfected into Platinum-E packaging cells using FuGENE 6 transfection reagent (Roche). The cell culture supernatants were harvested 48 h after transfection, supplemented with 5 µg/ml polybrene and 10 ng/ml Flt3 ligand, and used to infect BM-derived pDCs. After centrifugation at 2,000 rpm for 1 h, plates were incubated for 8 h at 32°C and for 16 h at 37°C. Before assay, two additional retroviral infections were performed at daily intervals.

F-actin localization. After fixation with 4% paraformaldehyde, cells were treated with 0.1% saponin in PBS containing 0.1% BSA and stained with Alexa Fluor 488–conjugated phalloidin (Invitrogen). For preparation of immobilized CpG-A microsphere, 10⁶ FluoSpheres polystyrene microsphere beads (10 µm; Invitrogen) were coated with 100 µM CpG-A overnight and washed five times with PBS containing 0.1% BSA. All images were taken with a laser-scanning confocal microscope (LSM 510 META; Carl Zeiss, Inc.).

Pulldown assay, immunoblotting, and in vitro kinase assay. To assess Rac activation, aliquots of the cell extracts were kept for total lysate controls, and the remaining extracts were incubated with glutathione-S-transferase fusion Rac-binding domain of PAK1 at 4°C for 60 min. The bound proteins and the same amounts of total lysates were analyzed by SDS-PAGE, and blots were probed with anti-Rac antibody (23A8; Millipore). Activation of STAT-1, Akt, ERK, JNK, p38, or IKK-α was analyzed by immunoblot with the phosphospecific antibody for STAT-1 (Tyr701; 9171; Cell Signaling Technology), Akt (Ser473; 9271; Cell Signaling Technology), ERK (Tyr204; sc-7383; Santa Cruz Biotechnology, Inc.), JNK (Thr183/Tyr185; 9255; Cell Signaling Technology), p38 (Thr180/Tyr182; 9211; Cell Signaling Technology), or IKK-α (Ser176/180; 2697; Cell Signaling Technology), respectively. In some experiments, cells were treated before stimulation with bacterially produced Tat–T17N-Rac or Tat–WT Rac. For in vitro kinase assay, cell lysates were immunoprecipitated with anti-IRAK1 antibody (06–872; Millipore). The immunoprecipitates were incubated for 30 min at 30°C in kinase buffer (20 mM Hepes, pH 7.6, 10 mM MgCl₂, 2 mM MnCl₂, 50 mM NaCl, 0.5 µM ATP, 10 µCi γ–³²P ATP, 0.1 mM Na₃VO₄, 10 mM β–glycerophosphate, 10 mM p-nitrophenyl phosphate, 1 mM DTT, 10 mM NaF, and complete protease inhibitor). Samples were washed with lysis buffer (20 mM Tris-HCl, pH 8.0, 150 mM NaCl, 5 mM EDTA, 1 mM PMSF, 20 µg/ml aprotinin, 10 mM NaF, 10 mM β-glycerophosphate, 1 mM Na₃VO₄, and 1% NP-40) and then subjected to SDS-PAGE and autoradiography.

Immunofluorescence microscopy. To assess subcellular localization of TLR9, fixed cells were made permeable for 5 min with 0.2% (vol/vol) Triton X-100 and were stained with anti-TfR antibody (C2; BD) or anti–LAMP-1 antibody (1D4B; BD), followed by Alexa Fluor 546–conjugated anti–rat IgG antibody (Invitrogen). In some experiments, cells were treated with

ER–Tracker Red (Invitrogen). The DeltaVision Restoration Microscopy system (Applied Precision) with a 60× objective attached to a cooled charge-coupled device camera was used for microscopy. Images were acquired with the DeltaVision SoftWorX Resolve 3D capture program and were collected as a stack of 0.2-µm increments. After deconvolution, images were viewed as a single section on the z axis. The area of TLR9 or CpG DNA (CpG-A or CpG-B) localized together with TfR, LAMP-1, or ER–Tracker was calculated in each cell using the MetaMorph imaging system (Universal Imaging). The percentage of colocalization was determined by dividing the area of TLR9 or CpG DNA localized together with TfR, LAMP-1, or ER-Tracker by the total area of TLR9 or CpG DNA, respectively.

To examine the nuclear translocation of IRF-7, fixed cells were permeabilized for 5 min with 0.5% (wt/vol) saponin (Sigma-Aldrich). After being blocked with 20% goat serum for 30 min, cells were stained with anti–IRF-7 antibody (Invitrogen) at 4°C overnight and incubated with biotin-conjugated anti–rabbit IgG (Jackson ImmunoResearch Laboratories) followed by Alexa Fluor 488–conjugated streptavidin (Molecular Probes). The cells were washed and mounted using fluorescent mounting medium (Dako) with DAPI (Wako Chemicals USA, Inc.). All images were taken with a laser-scanning confocal microscope (LSM 510 META).

Real-time PCR. After treatment with RNase-free DNase I (Invitrogen), RNA samples were reverse transcribed with random primers (Invitrogen) and SuperScript III reverse transcriptase (Invitrogen). Quantitative real-time RT-PCR analysis was performed using specific primers (TaqMan Gene Expression Assays; Applied Biosystems).

Reporter assay. Reporter assay was performed as described elsewhere (Hoshino et al., 2006). In brief, 293T cells were seeded on a 24-well plate (7 × 10⁴ cells per well). The next day, these cells were transfected with 56 ng of luciferase reporter plasmid alone or together with a combination of the expression plasmid for MyD88 (65.6 ng), IRF-7 (216.8 ng), or IKK-α and its mutants (228 or 456 ng). Cell lysates were prepared 24 h after transfection and luciferase activity was measured by the Dual-luciferase reporter assay system (Promega).

Statistical analysis. P-values were calculated using the two-tailed Student's *t* test.

Online supplemental material. Fig. S1 shows the effect of CXCL16 deficiency, pertussis toxin, or PP2 on CpG-A uptake, actin polymerization, and cytokine production in pDCs. Fig. S2 shows that DOCK2 deficiency does not affect CpG-A–induced actin polymerization and Rac activation in myeloid DCs. Fig. S3 shows that DOCK2 deficiency does not alter subcellular localization of TLR9 and CpG-B in pDCs. Fig. S4 shows that the serine phosphorylation of IKK-α at position 176/180 is critical for IRF-7–mediated type I IFN induction. Online supplemental material is available at http://www.jem.org/cgi/content/full/jem.20091776/DC1.

REFERENCES

Akira, S., S. Uematsu, and O. Takeuchi. 2006. Pathogen recognition and innate immunity. *Cell.* 124:783–801. doi:10.1016/j.cell.2006.02.015

Blanco, P., A.K. Palucka, M. Gill, V. Pascual, and J. Banchereau. 2001. Induction of dendritic cell differentiation by IFN-α in systemic lupus erythematosus. *Science.* 294:1540–1543. doi:10.1126/science.1064890

Brugnera, E., L. Haney, C. Grimsley, M. Lu, S.F. Walk, A.-C. Tosello-Trampont, I.G. Macara, H. Madhani, G.R. Fink, and K.S. Ravichandran. 2002. Unconventional Rac-GEF activity is mediated through the Dock180-ELMO complex. *Nat. Cell Biol.* 4:574–582.

Cammarano, M.S., and A. Minden. 2001. Dbl and the Rho GTPases activate NF κ B by I κ B kinase (IKK)-dependent and IKK-independent pathways. *J. Biol. Chem.* 276:25876–25882. doi:10.1074/jbc.M011345200

Côté, J.-F., and K. Vuori. 2002. Identification of an evolutionarily conserved superfamily of DOCK180-related proteins with guanine nucleotide exchange activity. *J. Cell Sci.* 115:4901–4913. doi:10.1242/jcs.00219

Diebold, S.S., T. Kaisho, H. Hemmi, S. Akira, and C. Reis e Sousa. 2004. Innate antiviral responses by means of TLR7-mediated recognition of single-stranded RNA. *Science.* 303:1529–1531. doi:10.1126/science.1093616

Ehrhardt, C., C. Kardinal, W.J. Wurzer, T. Wolff, C. von Eichel-Streiber, S. Pleschka, O. Planz, and S. Ludwig. 2004. Rac1 and PAK1 are upstream of IKK-ε and TBK-1 in the viral activation of interferon regulatory factor-3. *FEBS Lett.* 567:230–238. doi:10.1016/j.febslet.2004.04.069

Fukui, Y., O. Hashimoto, T. Sanui, T. Oono, H. Koga, M. Abe, A. Inayoshi, M. Noda, M. Oike, T. Shirai, and T. Sasazuki. 2001. Haematopoietic cell-specific CDM family protein DOCK2 is essential for lymphocyte migration. *Nature.* 412:826–831. doi:10.1038/35090591

Gilliet, M., W. Cao, and Y.-J. Liu. 2008. Plasmacytoid dendritic cells: sensing nucleic acids in viral infection and autoimmune diseases. *Nat. Rev. Immunol.* 8:594–606. doi:10.1038/nri2358

Gotoh, K., Y. Tanaka, A. Nishikimi, A. Inayoshi, M. Enjoji, R. Takayanagi, T. Sasazuki, and Y. Fukui. 2008. Differential requirement for DOCK2 in migration of plasmacytoid dendritic cells versus myeloid dendritic cells. *Blood.* 111:2973–2976. doi:10.1182/blood-2007-09-112169

Guiducci, C., G. Ott, J.H. Chan, E. Damon, C. Calacsan, T. Matray, K.-D. Lee, R.L. Coffman, and F.J. Barrat. 2006. Properties regulating the nature of the plasmacytoid dendritic cell response to Toll-like receptor 9 activation. *J. Exp. Med.* 203:1999–2008. doi:10.1084/jem.20060401

Guiducci, C., C. Ghirelli, M.-A. Marloie-Provost, T. Matray, R.L. Coffman, Y.-J. Liu, F.J. Barrat, and V. Soumelis. 2008. PI3K is critical for the nuclear translocation of IRF-7 and type I IFN production by human plasmacytoid predendritic cells in response to TLR activation. *J. Exp. Med.* 205:315–322. doi:10.1084/jem.20070763

Gursel, M., I. Gursel, H.S. Mostowski, and D.M. Klinman. 2006. CXCL16 influences the nature and specificity of CpG-induced immune activation. *J. Immunol.* 177:1575–1580.

Häcker, H., and M. Karin. 2006. Regulation and function of IKK and IKK-related kinases. *Sci. STKE.* 2006:re13. doi:10.1126/stke.3572006re13

Heil, F., H. Hemmi, H. Hochrein, F. Ampenberger, C. Kirschning, S. Akira, G. Lipford, H. Wagner, and S. Bauer. 2004. Species-specific recognition of single-stranded RNA via toll-like receptor 7 and 8. *Science.* 303:1526–1529. doi:10.1126/science.1093620

Hemmi, H., O. Takeuchi, T. Kawai, T. Kaisho, S. Sato, H. Sanjo, M. Matsumoto, K. Hoshino, H. Wagner, K. Takeda, and S. Akira. 2000. A Toll-like receptor recognizes bacterial DNA. *Nature.* 408:740–745. doi:10.1038/35047123

Hemmi, H., T. Kaisho, O. Takeuchi, S. Sato, H. Sanjo, K. Hoshino, T. Horiuchi, H. Tomizawa, K. Takeda, and S. Akira. 2002. Small anti-viral compounds activate immune cells via the TLR7 MyD88-dependent signaling pathway. *Nat. Immunol.* 3:196–200. doi:10.1038/ni758

Honda, K., Y. Ohba, H. Yanai, H. Negishi, T. Mizutani, A. Takaoka, C. Taya, and T. Taniguchi. 2005a. Spatiotemporal regulation of MyD88-IRF-7 signalling for robust type-I interferon induction. *Nature.* 434:1035–1040. doi:10.1038/nature03547

Honda, K., H. Yanai, H. Negishi, M. Asagiri, M. Sato, T. Mizutani, N. Shimada, Y. Ohba, A. Takaoka, N. Yoshida, and T. Taniguchi. 2005b. IRF-7 is the master regulator of type-I interferon-dependent immune responses. *Nature.* 434:772–777. doi:10.1038/nature03464

Honda, K., A. Takaoka, and T. Taniguchi. 2006. Type I interferon [corrected] gene induction by the interferon regulatory factor family of transcription factors. *Immunity.* 25:349–360. doi:10.1016/j.immuni.2006.08.009

Hoshino, K., T. Sugiyama, M. Matsumoto, T. Tanaka, M. Saito, H. Hemmi, O. Ohara, S. Akira, and T. Kaisho. 2006. IkappaB kinase-α is critical for

interferon-α production induced by Toll-like receptors 7 and 9. *Nature.* 440:949–953. doi:10.1038/nature04641

Jarrossay, D., G. Napolitani, M. Colonna, F. Sallusto, and A. Lanzavecchia. 2001. Specialization and complementarity in microbial molecule recognition by human myeloid and plasmacytoid dendritic cells. *Eur. J. Immunol.* 31:3388–3393. doi:10.1002/1521-4141(200111)31:11<3388::AID-IMMU3388>3.0.CO;2-Q

Kawai, T., S. Sato, K.J. Ishii, C. Coban, H. Hemmi, M. Yamamoto, K. Terai, M. Matsuda, J. Inoue, S. Uematsu, et al. 2004. Interferon-α induction through Toll-like receptors involves a direct interaction of IRF7 with MyD88 and TRAF6. *Nat. Immunol.* 5:1061–1068. doi:10.1038/ni1118

Krieg, A.M., A.-K. Yi, S. Matson, T.J. Waldschmidt, G.A. Bishop, R. Teasdale, G.A. Koretzky, and D.M. Klinman. 1995. CpG motifs in bacterial DNA trigger direct B-cell activation. *Nature.* 374:546–549. doi:10.1038/374546a0

Kunisaki, Y., A. Nishikimi, Y. Tanaka, R. Takii, M. Noda, A. Inayoshi, K.-i. Watanabe, F. Sanematsu, T. Sasazuki, T. Sasaki, and Y. Fukui. 2006. DOCK2 is a Rac activator that regulates motility and polarity during neutrophil chemotaxis. *J. Cell Biol.* 174:647–652. doi:10.1083/jcb.200602142

Lande, R., J. Gregorio, V. Facchinetti, B. Chatterjee, Y.-H. Wang, B. Homey, W. Cao, Y.-H. Wang, B. Su, F.O. Nestle, et al. 2007. Plasmacytoid dendritic cells sense self-DNA coupled with antimicrobial peptide. *Nature.* 449:564–569. doi:10.1038/nature06116

Latz, E., A. Schoenemeyer, A. Visintin, K.A. Fitzgerald, B.G. Monks, C.F. Knetter, E. Lien, N.J. Nilsen, T. Espevik, and D.T. Golenbock. 2004. TLR9 signals after translocating from the ER to CpG DNA in the lysosome. *Nat. Immunol.* 5:190–198. doi:10.1038/ni1028

Leifer, C.A., M.N. Kennedy, A. Mazzoni, C. Lee, M.J. Kruhlak, and D.M. Segal. 2004. TLR9 is localized in the endoplasmic reticulum prior to stimulation. *J. Immunol.* 173:1179–1183.

Lund, J., A. Sato, S. Akira, R. Medzhitov, and A. Iwasaki. 2003. Toll-like receptor 9–mediated recognition of Herpes simplex virus-2 by plasmacytoid dendritic cells. *J. Exp. Med.* 198:513–520. doi:10.1084/jem.20030162

Nestle, F.O., C. Conrad, A. Tun-Kyi, B. Homey, M. Gombert, O. Boyman, G. Burg, Y.-J. Liu, and M. Gilliet. 2005. Plasmacytoid predendritic cells initiate psoriasis through interferon-α production. *J. Exp. Med.* 202:135–143. doi:10.1084/jem.20050500

Nishikimi, A., H. Fukuhara, W. Su, T. Hongu, S. Takasuga, H. Mihara, Q. Cao, F. Sanematsu, M. Kanai, H. Hasegawa, et al. 2009. Sequential regulation of DOCK2 dynamics by two phospholipids during neutrophil chemotaxis. *Science.* 324:384–387. doi:10.1126/science.1170179

Nombela-Arrieta, C., R.A. Lacalle, M.C. Montoya, Y. Kunisaki, D. Megías, M. Marqués, A.C. Carrera, S. Mañes, Y. Fukui, C. Martínez-A, and J.V. Stein. 2004. Differential requirements for DOCK2 and phosphoinositide-3-kinase γ during T and B lymphocyte homing. *Immunity.* 21:429–441. doi:10.1016/j.immuni.2004.07.012

Nombela-Arrieta, C., T.R. Mempel, S.F. Soriano, I. Mazo, M.P. Wymann, E. Hirsch, C. Martínez-A, Y. Fukui, U.H. von Andrian, and J.V. Stein. 2007. A central role for DOCK2 during interstitial lymphocyte motility and sphingosine-1-phosphate–mediated egress. *J. Exp. Med.* 204:497–510. doi:10.1084/jem.20061780

Oakley, F.D., D. Abbott, Q. Li, and J.F. Engelhardt. 2009. Signaling components of redox active endosomes: the redoxosomes. *Antioxid. Redox Signal.* 11:1313–1333. doi:10.1089/ars.2008.2363

Reif, K., and J.G. Cyster. 2002. The CDM protein DOCK2 in lymphocyte migration. *Trends Cell Biol.* 12:368–373. doi:10.1016/S0962-8924(02)02330-9

Sanjuan, M.A., N. Rao, K.T. Lai, Y. Gu, S. Sun, A. Fuchs, W.-P. Fung-Leung, M. Colonna, and L. Karlsson. 2006. CpG-induced tyrosine phosphorylation occurs via a TLR9-independent mechanism and is required for cytokine secretion. *J. Cell Biol.* 172:1057–1068. doi:10.1083/jcb.200508058

Shimaoka, T., K.-i. Seino, N. Kume, M. Minami, C. Nishime, M. Suematsu, T. Kita, M. Taniguchi, K. Matsushima, and S. Yonehara. 2007. Critical role for CXC chemokine ligand 16 (SR-PSOX) in Th1 response mediated by NKT cells. *J. Immunol.* 179:8172–8179.

Shulman, Z., R. Pasvolsky, E. Woolf, V. Grabovsky, S.W. Feigelson, N. Erez, Y. Fukui, and R. Alon. 2006. DOCK2 regulates chemokine-triggered lateral lymphocyte motility but not transendothelial migration. *Blood*. 108:2150–2158. doi:10.1182/blood-2006-04-017608

Uematsu, S., S. Sato, M. Yamamoto, T. Hirotani, H. Kato, F. Takeshita, M. Matsuda, C. Coban, K.J. Ishii, T. Kawai, et al. 2005. Interleukin-1 receptor-associated kinase-1 plays an essential role for Toll-like receptor (TLR)7- and TLR9-mediated interferon-α induction. *J. Exp. Med.* 201:915–923. doi:10.1084/jem.20042372

Verthelyi, D., K.J. Ishii, M. Gursel, F. Takeshita, and D.M. Klinman. 2001. Human peripheral blood cells differentially recognize and respond to two distinct CPG motifs. *J. Immunol.* 166:2372–2377.